Femtosecond control of photoionization and photodissociation of sodium iodine molecules by laser pulse

Xiaoguang Ma (马晓光), Chuanlu Yang (杨传路), Meishan Wang (王美山), Yubing Gong (龚玉兵), and Wenwang Liu (刘文旺)

School of Physics and Optoelectronic Engineering, Ludong University, Yantai 264025, China

**Corresponding author: hsiaoguangma@188.com*

Received March 29, 2012; accepted May 17, 2012; posted online September 28, 2012

Wave packet propagation techniques are used to find experimentally reliable laser parameters that yield optimal production. The photoionization and photodissociation dynamics of sodium iodine molecules are interpreted into several channels. Several frequencies are found to be suitable for NaI molecules during the photoionization and dissociation processes. Photon-dressed excited states and electron-dressed ionic continuum states facilitate the search for available laser parameters.

OCIS codes: 020.7010, 300.2530, 140.7010.

doi: 10.3788/COL201210.110201.

The quantum control of transition is now possible, and optimized techniques for achieving desired outcomes are currently available[1−8]. The ultrafast photo-dynamics of a chemical reaction, such as the direct dissociation process, has been observed in recent years with the development of increasingly short laser pulses with durations of several femtoseconds[2−6]. Likewise, it is now possible to monitor elementary chemical and physical processes, such as the reaction dynamic process[9], the electron transport process[9−11], the ultra-cold dynamic process[12,13] in molecules, the photoionization micro-mechanisms of atoms under the condensed conditions[14−22] and the biophysical processes in organic bodies[23] as a function of time on a femtosecond or picosecond time scale. Moreover, real-time femtosecond transition state spectroscopy in dissociation processes that allows bond breaks to be observed has also become a reality[1−8]. The laser pump-probe technique has become a powerful method used in studying the dynamic processes. In the laser pump-probe technique, the single or multi-photon excitation scheme prepares an excited state, and an additional photon from the same or from an independently tunable source ionizes the excited state[1−8,24−33]. The pump pulse triggers the dynamics, and the probe pulse records snapshots of the ultrafast processes at times set by the time delay between the two pulses[1−9]. The transition states depend on the position of the wave packet on the excited potential energy surface; in turn, these provide information about the dissociation processes involved[1−8,24−33].

Two sequential coherent laser pulses control the ionization and dissociation reaction process of sodium iodine molecules, forming sodium and iodine atoms by exciting the reactants in the transition state through a two-step process[5]. Since the first dynamical study of the NaI molecule on a femtosecond time scale by Rose *et al.* in 1988[3,4], numerous experimental and theoretical research on the system have been performed[24−30]. Many factors influence the experiments and the accurate potentials of the electronic states of molecules. Therefore, theoretical studies must choose suitable parameters in the experiments. In this letter, we develop a theoretical scheme that searches for suitable parameters.

The femtosecond pulse, time-resolved photodissociation, and photoionization processes of NaI are simulated using the time-dependent wave packet method[31,32]. Sodium iodide is a classic example of a diatomic molecule. The femtosecond pump-probe study conducted by Zewail provides insights into dissociation dynamics[29]. For sodium iodide, all available calculations of quantum control are performed for only a single probe wavelength. The accurate treatments of the photoionization and dissociation dynamics of NaI are scarce. Thus, we create a well-defined quantum mechanical wave-packet using a short laser pulse on a molecule in its equilibrium state. We then used another probe pulse to study the dissociation and ionization processes (Fig. 1). Aside from the typical frequency used, we find that several frequencies can be applied to molecule that, in turn, can be used to enhance or control chemical reactions through the careful application of pulses of light with optimal frequencies, intensities, durations, and timings[33].

Figure 1 shows the schematic representation of the photon-induced ionization and dissociation processes of molecular NaI. The potential energy curves for the low-lying and the ionic ground electronic states were calculated using the well-known Molpro package. The combination of pump and probe laser pulses reveals the nature of the initial photon absorption step and the subsequent dissociation processes. The entire NaI molecule is distributed on the ground electronic state $X^1\Sigma^+$ (Figs. 1 and 2). When the pump pulse triggers the dynamics at time $t = 0$, the population declines from the $X^1\Sigma^+$ to $A^1\Sigma^+$ states, until the steady state at approximately $t = 150$ fs. The molecule then starts to populate from the $A^1\Sigma^+$ to $I^2\Sigma^+$ ionic states when the other pulse occurs at approximately $t = 250$ fs. The ultra-short pulses then prepare a particular state of the system, and trigger some characteristic dynamic behaviors. Using the aforementioned technique, we studied the pho-

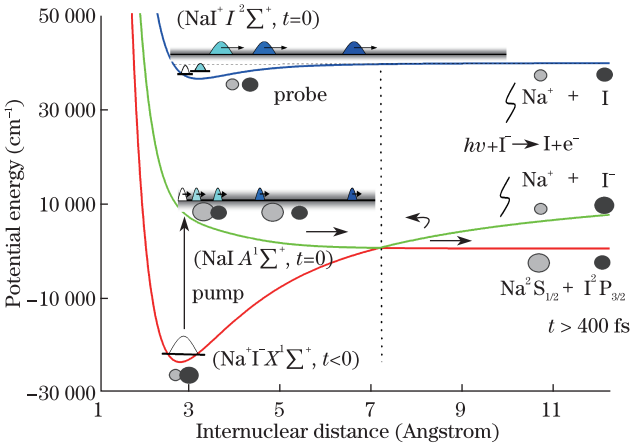

Fig. 1. Schematic representation of the dynamics on the potential energy surfaces of NaI, the ground state $X^1\Sigma^+$, the excited state $A^1\Sigma^+$, and the ionic state $I^2\Sigma^+$. The snapshots of the photodissociation and femtosecond photoionization processes at different delay time as well as the distance between Na and I atoms are also shown.

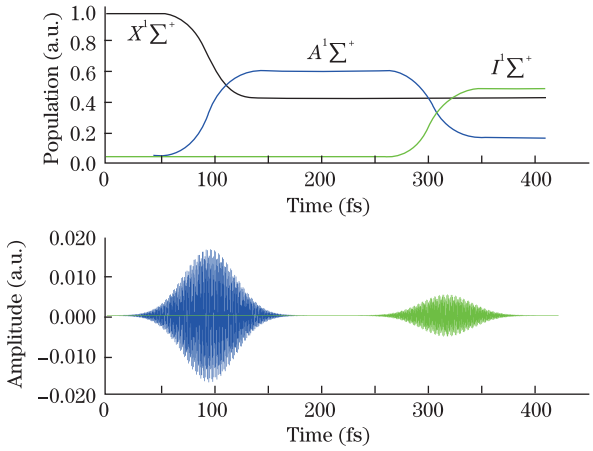

Fig. 2. Population pumping scheme of NaI on three electronic states using 2-fs laser pulses.

todissociation processes [$Na^+I^-(X^1\Sigma^+) \rightarrow Na^+ + I^-$, $NaI(A^1\Sigma^+) \rightarrow Na(^2S_{1/2}) + I(^2P_{3/2})$] and photoionization processes [$NaI^+(I^2\Sigma^+) + e^- \rightarrow Na^+ + I + e^-$ or $I^- \rightarrow I + e^-$] shown in Fig. 1.

The time-dependent Schrodinger equation must first be solved in order to study the dynamic processes on a femtosecond scale. Engholm[33] reported the time-dependent formulation for nuclear dynamics in molecules induced by electronic excitation in a radiation field. When a molecule interacts with a radiation field, the time evolution of the molecular states is given by the following time-dependent Schrödinger equation[33]:

$$\mathrm{i}h\frac{\partial\left|\psi\left(R,r,t\right)\right\rangle}{\partial t} = \widehat{H}\left|\psi\left(R,r,t\right)\right\rangle, \tag{1}$$

where r and R denote the electronic and nuclear coordinates, respectively. The total Hamiltonian $\widehat{H}$ includes the molecular Hamiltonian $\widehat{H}_{\mathrm{mol}}$ and the external electric field interaction $\widehat{H}_{\mathrm{I}}(t)$. The total Hamiltonian $\widehat{H}$ is

$$\widehat{H} = \widehat{H}_{\mathrm{mol}} + \widehat{H}_I(t). \tag{2}$$

For actual calculations, $\widehat{H}_{\mathrm{mol}}$ is separated in the adiabatic representation as

$$\widehat{H}_{\mathrm{mol}} = \widehat{T}_{\mathrm{N}}(R) + \widehat{H}_{\mathrm{el}}(R;r). \tag{3}$$

Within the dipole approximation, the term$\widehat{H}_{\mathrm{I}}(t)$ is calculated as

$$\widehat{H}_I(t) = -\widehat{d}\,\overset{1}{E}_0\cos\omega t, \tag{4}$$

where $\widehat{d}$ is the dipole electric operator of the molecule, and $\overset{1}{E}_0 = E_0(t)\overset{r}{e}$ is the electric field vector along polarization $\overset{1}{e}$. In addition, $|\psi(R,r,t)\rangle$ is the state vector of molecule at time t, and is obtained as

$$|\psi(R,r,t)\rangle = \sum_{i=1}^{n}\chi_i(R,t)\phi_i(r;R), \tag{5}$$

where $\phi_i(r;R)$ is an electronic eigenstate obtained for fixed values R from the following eigenequation:

$$\widehat{H}_{el}(R;r)\phi_i(r;R) = E_i(R)\phi_i(r;R), \tag{6}$$

and $\chi_i(R,t)$ is a vibrational-rotational eigenstate in the i electronic eigenstate. The population variation of NaI in one electronic state $X^1\Sigma^+$ (Fig. 3) was studied using $||\psi(R,r,t)\rangle|^2$ in the wavepacket form when the first pulse was applied to the molecule earlier shown in Fig. 2. If the pump pulse time was long enough, the population was entirely pumped into the upper electronic state.

By substituting Eq. (6) into Eq. (1) in the NaI molecule cases, the time-dependent Schrodinger equation can be written as

$$\mathrm{i}h\frac{\partial}{\partial t}\begin{vmatrix}\chi_X(R,t)\\ \chi_A(R,t)\\ \chi_{I_1}(R,t)\\ M\\ \chi_{I_n}(R,t)\end{vmatrix} = \begin{vmatrix}\widehat{H}_{XX} & \widehat{H}_{XA} & 0 & 0 & 0\\ \widehat{H}_{AX} & \widehat{H}_{AA} & \widehat{H}_{AI} & 0 & \widehat{H}_{IA}\\ 0 & \widehat{H}_{AI} & \widehat{H}_{II}+E_{I,1} & 0 & 0\\ M & M & M & M & M\\ 0 & \widehat{H}_{IA} & 0 & 0 & \widehat{H}_{II}+E_{I,n}\end{vmatrix}\begin{vmatrix}\chi_X(R,t)\\ \chi_A(R,t)\\ \chi_{I_1}(R,t)\\ M\\ \chi_{I_n}(R,t)\end{vmatrix}, \tag{7}$$

where $\chi_X(R,t)$ and $\chi_A(R,t)$ denote the wave functions of the ground state $X^1\Sigma^+$ and the exited state $A^1\Sigma^+$ of the nuclei of neutral NaI molecules, respectively. $|\chi_{I_n}(R,t)\rangle(n$=1–50) denotes the wavefunction of the quasi-continuum states of the ionic NaI molecule. The diagonal element can be expressed as

$$\widehat{H}_{II} = -\frac{h^2}{2m}\frac{\partial^2}{\partial R^2} + E_i(R). \tag{8}$$

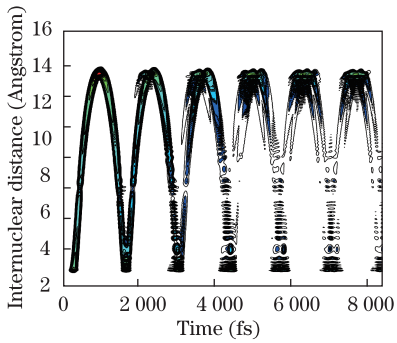

Fig. 3. Variations of the population of NaI in the $X^1\Sigma^+$ electronic state as a function of time.

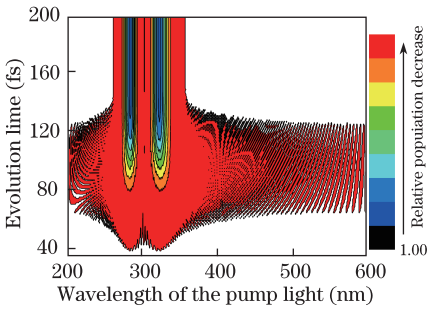

Fig. 4. Evolution of the population of NaI on $A^1\Sigma^+$ state at different wavelengths after the pump pulse. The population pumped onto $A^1\Sigma^+$ state has 2 maximum signals at laser wavelengths of approximately 283 and 312 nm, respectively.

The off-diagonal element is expressed as

$$\widehat{H}_{IJ} = \mu_{IJ}E(t). \tag{9}$$

The matrix equation is solved using the split operator Fourier method[34]. In the adiabatic representation, the wave packets are initialized as

$$\begin{cases} |\chi_X(R, t=0)\rangle = |\phi_\upsilon\rangle \\ |\chi_A(R, t=0)\rangle = 0 \\ |\chi_I(R, t=0)\rangle = 0 \end{cases}, \tag{10}$$

where $|\phi_\upsilon\rangle$ is usually the ground vibrational eigenfunction of the ground electronic state corresponding to the vibrational quantum number υ. Using Eq. (7), under the diabatic representation with a diagonal kinetic energy operator for the nuclear motion, the couplings are restricted to the off-diagonal elements of the potential energy matrix. The restriction of the couplings is more convenient for numerical calculations, because the dynamic revolution processes of ionization and dissociation in NaI molecules can be studied on a femtosecond scale.

The coupled channel equations were solved by the split-operator method, which employed a symmetric splitting of the kinetic and potential energy operators. A 1 024-point space grid in [2.0, 15.0] atomic units was used to represent the wave functions on the three potential curves. The probability in each dissociative channel was obtained by integrating the corresponding flux over the time interval in which it was recorded. Then, an absorbing potential was placed at an inter-nuclear separation of $R > 15.0$ au to avoid wave packet reflection from the grid boundaries. The full-width at half-maximum (FWHM) intensities of the pump and probe pulses were both 40 fs. Therefore, only few vibrational energy levels of NaI were included. The delay time between the two pulses is 200 fs. The intensities of the pump and probe pulses are 1.0×10^{13} and 1.0×10^{12} W/cm^2, respectively.

A previous NaI excitation experiment[46] used laser pump wavelengths of 300, 310, and 328 nm. The 310-nm wavelength has been obtained from the difference between the corresponding potentials used. The obtained difference between the potentials of $A^1\Sigma^+$ and $X^1\Sigma^+$ is 312 nm and pumped the largest population to the $X^1\Sigma^+$ electronic state. Another experiment also used a wavelength of 312 nm[30]. In this letter, we observed another strong signal when a 283-nm wavelength laser pulse is applied to the $X^1\Sigma^+$ state. In the region between the 271- and 362-nm wavelengths, the population of NaI is distributed onto the $A^1\Sigma^+$ state and remained steady (Fig. 4). The laser pulse within the wavelength regions efficiently populate the NaI molecules onto the excited state $A^1\Sigma^+$. Further, the 283- and 312-nm laser pulses pumped the maximum population onto the excited states. Wider and more accurate wavelengths can be chosen from the wavelength region between 271 and 362 nm. Therefore, more wavelengths are usable in the experiments.

Figure 5 shows the evolution of the NaI population on the excited state $A^1\Sigma^+$ at different laser wavelengths after the probe pulse at 280 fs. Several regions of the laser wavelength efficiently triggered the photoionization process. Increased amounts of short laser wavelengths populated the NaI molecules onto more high-energy ionic states, and less ionic continuum states are included. In the region between 365 and 435 nm, the NaI molecules are promoted onto some excited vibrational states and lower-lying continuum states; therefore, the region is wider. Different probe states must use different laser wavelengths. If the ground or some low-lying states are probed, the wavelength becomes longer. Previous experiments have used probe lasers with wavelengths of at least 600 nm[35].

Figure 6 shows all the available wavelengths for pump and probe laser pulses. As can be seen, the wavelength primarily depends on the difference between the potentials of $A^1\Sigma^+$ and $X^1\Sigma^+$ for photodissociation processes. Photoionization processes, meanwhile, depend on the difference between the potentials of the$A^1\Sigma^+$ and $I^2\Sigma^+$ states; however, the latter depends on the energy of the photo-electrons. In the experiment, we used 52 potentials of the $I^2\Sigma^+$state from the photo-electronic energies ranging from 0 to 5 eV. All the wavelengths in each band were available for the femtosecond dissociation and ionization processes of NaI molecules. The states or regions are called the electron-dressed ionic $I^2\Sigma^+$ states and photon-dressed excited states $A^1\Sigma^+$. The states aid in the study of femtosecond processes.

In conclusions, the photodissociation dynamics of sodium iodide are theoretically studied using the time-dependent wave packet method. The transition states of NaI are modeled as a function of the probe wavelength for a wide region between 323 and 254 nm. The electronic state is called the photon-dressed excited state. Between the 271- and 362-nm wavelength region, the population of NaI is distributed onto the $A^1\Sigma^+$ state and remains steady. The laser pulse within the wavelength region

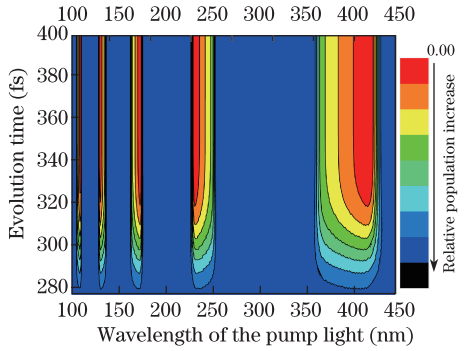

Fig. 5. Evolution of the population of NaI on the $A^1\Sigma^+$ state at different wavelengths after the probe pulse. Several wavelength regions efficiently triggered the photoionization process.

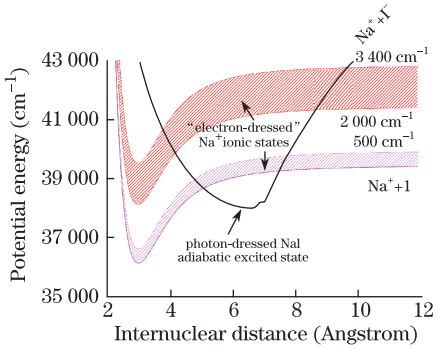

Fig. 6. Photon- and electron-dressed electronic states represent the available laser wavelength region used in preparing the particular states.

efficiently populates the NaI molecules onto the excited state $A^1\Sigma^+$. The 283- and 312-nm laser pulses pump the maximum population onto the excited states. Wider and more accurate wavelengths can be chosen from the region between 271 and 362 nm. Therefore, many wavelengths are considered usable in the experiments. Furthermore, several frequencies are found to be useful in the study of the photoionization and photodissociation processes of NaI molecules.

This work was supported by the Natural Science Foundation Project of the Shandong Province (No. ZR2011AM010) and the University Science and Technology Planning Program of Shandong Province (No. J10LB60).

References

1. B. H. Hosseini, H. R. Sadeghpour, and N. Balakrishnan, Phys. Rev. A **71,** 023402 (2005).
2. S. Y. Lee, W. T. Pollard, and R. A. Mathies, J. Chem. Phys. **90,** 6146 (1989).
3. T. S. Rose, M. J. Rosker, and A. H. Zewail, J. Chem. Phys. **88,** 6672 (1988).
4. M. J. Rosker, T. S. Rose, and A. H. Zewail, Chem. Phys. Lett. **146,** 175 (1988).
5. E. D. Potter, J. L. Herek, S. Pedersen, Q. Liu, and A. H. Zewail, Nature **355,** 66 (1992).
6. M. Dantus, M. J. Rosker, and A. H. Zewail, J. Chem. Phys. **87,** 2395 (1987).
7. M. J. Rosker, M. Dantus, and A. H. Zewail, Science **241,** 1200 (1988).
8. T. S. Rose, M. J. Rosker, and A. H. Zewail, J. Chem. Phys. **91,** 7415 (1989).
9. Y. P. An, C. L. Yang, M. S. Wang, X. G. Ma, and D. H. Wang, Curr. Appl. Phys. **10,** 260 (2010).
10. Y. P. An, C. L. Yang, M. S. Wang, X. G. Ma, and D. H. Wang, J. Chem. Phys. **131,** 024311 (2009).
11. Y. C. Li, C. L. Yang, M. Y. Sun, X. X. Li, Y. P. An, M. S. Wang, X. G. Ma, and D. H. Wang, J. Phys. Chem. 113, 1353 (2009).
12. X. F. Tong, C. L. Yang, Y. P. An, M. S. Wang, X. G. Ma, and D. H. Wang, J. Chem. Phys. **131,** 244304 (2009)
13. Y. P. An, C. L. Yang, M. S. Wang, X. G. Ma, and D. H. Wang, Acta Phys. Sin. **59,** 2010 (2010).
14. W. G. Sun, X. G. Ma, and Y. S. Cheng, Phys. Lett. A **326,** 243 (2004).
15. X. G. Ma, Phys. Lett. A **348,** 310 (2006).
16. X. G. Ma and W. G. Sun, Chin. Phys. **14,** 1792(2005).
17. X. G. Ma, W. G. Sun, and Y. S. Cheng, Acta Phy. Sin. **54,** 1149(2005).
18. X. G. Ma, W. G. Sun, and Y. S. Cheng, Commum. Theor. Phys. **43,** 159 (2005).
19. X. G. Ma, Y. B. Gong, M. S. Wang, and D. H. Wang, Phys. Lett. A **372,** 2274 (2008).
20. X. G. Ma, Y. B. Gong, and Z. J. Qu, Chin. Phys. B **18,** 1451 (2009).
21. X. G. Ma, C. L. Yang, Y. B. Gong, and M. S. Wang, Chin. Phys. B **18,** 5296 (2009).
22. X. G. Ma, Chin. Phys. B **18**, 161 (2009).
23. Y. B. Gong, B. Xu, X. G. Ma, Y. M. Dong, and C. L. Yang, J. Phys. Chem. C **111,** 4264 (2007).
24. P. Cong, A. Mokhtari, and A. H. Zewail, Chem. Phys. Lett. **172,** 109 (1990).
25. A. Materny, J. L. Herek, P. Cong, and A. H. Zewail, J. Phys. Chem. **98,** 3352 (1994).
26. J. L. Herek, A. Materny, and A. H. Zewail, Chem. Phys. Lett. **228,** 15 (1994).
27. V. H. Gregory, D. Qin, and H. L. Dai, J. Chem. Phys. **100,** 7832 (1996).
28. M. Motzkus, S. Pedersen, and A. H. Zewail, J. Phys. Chem. **100,** 5620 (1996).
29. A. H. Zewail, J. Phys. Chem. **97,** 12427 (1993).
30. E. Charron and A. S. Weiner, J. Chem. Phys. **108,** 3922 (1998).
31. H. Zhang, K. L. Han, Y. Zhao, G. He, and N. Lou, Chem. Phys. Lett. **271,** 204 (1997).
32. J. Hu, K. L. Han, and G. Z. He, Phys. Rev. Lett. **95,** 123001 (2005).
33. N. E. Henriksen, Theor. Chim. Acta. **82,** 249 (1992). J. Hu, K. L. Han, and G. Z. He, Phys. Rev. Lett. **95,** 123001 (2005).
34. R. Kosloff, J. Phys. Chem. **92,** 2087 (1988).
35. Volker Engel and H. Metiu, J. Chem. Phys. **91,** 1596 (1989).